

# Study on the Preparation and Strength-Ductility Mechanism of Layered Heterogeneous Magnesium Matrix Composites

Xiangyang Liu\*, Mingjie Shen

College of Mechanical & Electrical Engineering, Shaanxi University of Science & Technology, Xi'an, China  
Email: \*201905010614@sust.edu.cn

**How to cite this paper:** Liu, X.Y. and Shen, M.J. (2026) Study on the Preparation and Strength-Ductility Mechanism of Layered Heterogeneous Magnesium Matrix Composites. *World Journal of Engineering and Technology*, 14, 270-280.  
<https://doi.org/10.4236/wjet.2026.141016>

**Received:** December 26, 2025

**Accepted:** February 22, 2026

**Published:** February 25, 2026

Copyright © 2026 by author(s) and Scientific Research Publishing Inc.  
This work is licensed under the Creative Commons Attribution-NonCommercial International License (CC BY-NC 4.0).  
<http://creativecommons.org/licenses/by-nc/4.0/>



Open Access

## Abstract

In this study, carbon fiber (CF) reinforced magnesium matrix composites were used as the research object. Composites with micro-macro cross-scale layered configurations were designed and prepared by powder metallurgy sintering process. The tensile test results show that when the carbon fiber content is 1.2 wt.% and the thickness of the single-layer composite is 3.5 mm, the material exhibits excellent strength-ductility matching: the tensile strength is 269 MPa and the elongation at break is 14.7%, which achieves good plasticity while significantly improving the strength. The study further systematically analyzed the synergistic contribution of traditional strengthening mechanism and back stress strengthening to material strength, and revealed the improvement effect of carbon fiber on material plasticity through internal ductility mechanisms such as “pulling out”, as well as external energy dissipation pathways such as crack deflection. This work provides a new structural design idea for simultaneously improving the strength and ductility of magnesium matrix composites, and has important reference value for the optimization of its comprehensive mechanical properties.

## Keywords

Hierarchical Composites, Carbon Fiber, Mechanical Properties

## 1. Introduction

With the acceleration of industrialization and the continuous consumption of fossil energy, the problem of energy shortage has become increasingly prominent. Under the background of “double carbon” target, lightweight has become an inevitable trend [1]. Lightweight materials have significant potential in energy sav-

ing and emission reduction by reducing structural weight, and the demand for high strength and high plasticity lightweight materials is also increasing [2]. As the key development direction in the “Made in China 2025” and “14th Five-Year Plan”, high-performance light alloys (such as aluminum, magnesium, and titanium alloys) and carbon fiber composites are expected to continue to serve as key strategic materials during the “15th Five-Year Plan” and continue to promote industrial upgrading [3]. Taking the aviation field as an example, Boeing and Airbus have widely used magnesium (Mg) alloy die-castings in the economy seat frame to reduce the weight of the whole machine by hundreds of kilograms and greatly improve the fuel economy [4]. The good vibration reduction performance of magnesium alloy also improves the ride comfort. In recent years, with the development of rare earth magnesium alloys such as WE series, their heat resistance, strength and corrosion resistance have been significantly improved, and their application scenarios have gradually expanded from cabin structural parts to key harsh environments such as engine periphery and main drive system [5]. At the same time, new energy vehicles, aerospace equipment, medical equipment and other fields also put forward higher requirements for the performance of magnesium alloys.

Among various reinforcements, carbon fiber is considered to be an ideal choice to improve the performance of magnesium matrix composites due to its extremely high specific strength and specific modulus, excellent high temperature stability and extremely low (or negative) thermal expansion coefficient [6]. When introduced in the form of continuous fiber, it can effectively carry and transmit loads, so it has attracted much attention in the fields of aerospace, automotive and biomedical [7]. However, the preparation of such composites by traditional casting process faces significant challenges: the poor wettability of magnesium melt and carbon fiber can easily lead to harmful interface reactions, and lead to coarse matrix structure and porosity, resulting in weak interface bonding and insufficient matrix bearing, so that the performance of the composites is often lower than the theoretical expectation or even the matrix itself. At the same time, although nano-reinforcements such as carbon nanotubes can increase strength, they are often accompanied by a decrease in plasticity. Inspired by the multi-scale heterogeneous structure of natural biomaterials (such as bamboo and fish scales), bionic design provides a new idea for collaborative optimization of the strength, plasticity and interfacial properties of such composites, which is expected to achieve the unity of high performance and high reliability [8]. In 2022, Wang *et al.* constructed macroscopic layered composites and established a quantitative relationship between back stress and macroscopic work hardening behavior. Therefore, this structure is an ideal system to study the stress-strain relationship [9].

In this paper, CF was used as reinforcement material, and layered CF and Mg (CF/Mg) composites were prepared by ball milling mixture, “bottom-up” assembly and hot-pressing sintering technology. The effects of hot-pressing sintering process (sintering temperature, sintering time, sintering pressure) on the

microstructure/properties evolution of layered CF/Mg composites were studied. Combined with tensile test, the strengthening and ductility mechanism and strength/plasticity coexistence mechanism of layered CF/Mg composites were further revealed.

## 2. Experiments and Methods

### 2.1. Design and Characterization of Layered Composites

The magnesium powder (99.9% purity, 200 mesh) used in the experiment was purchased from Tangshan Wei Hao Company, China. The chopped carbon fiber (CF) was provided by Chengdu Organic Chemical Co., Ltd. Firstly, CF was put into a beaker containing anhydrous ethanol, and then it was placed in an ultrasonic cleaning machine for vibration for 2 h with a power of 150 W. The CF suspension was put into a drying oven at 55°C for 24 h. The dried CF and Mg alloy powder were mixed according to the mass fraction of 1.2 wt.%, and the mixed powder was put into the self-designed zirconium dioxide lining vacuum ball milling tank again. The ball milling powder was mixed with nitrogen as the protective atmosphere, so that the CF and Mg powder were mixed at a ball-to-powder ratio of 20:1. Zirconium dioxide ball was used as the grinding medium. The ball milling was started clockwise. After 1 h of each ball milling, the equipment stopped running for 10 min and changed the direction of motion. After 6 h, the mixed powder after ball milling was obtained. The raw materials and morphology are shown in **Figure 1**. Then, the obtained magnesium alloy powder and composite powder were alternately stacked in a  $\phi 45$  mm cylindrical graphite mold. After the powder laying of each layer is completed, the powder billet is compacted and flattened under the action of a press. Finally, a  $\phi 45$  mm cylindrical layered CF/Mg preform is obtained. After the blanking of the billet, the hot-pressing sintering was carried out at a pressure of 12 MPa, and the sintering temperature was set to 530°C. The whole process of hot-pressing sintering is in vacuum, and the sintering time is 50 min. The sintered samples were machined and the surface was refined to obtain a cylindrical sample with a target specification (diameter 45 mm, height 15 mm).

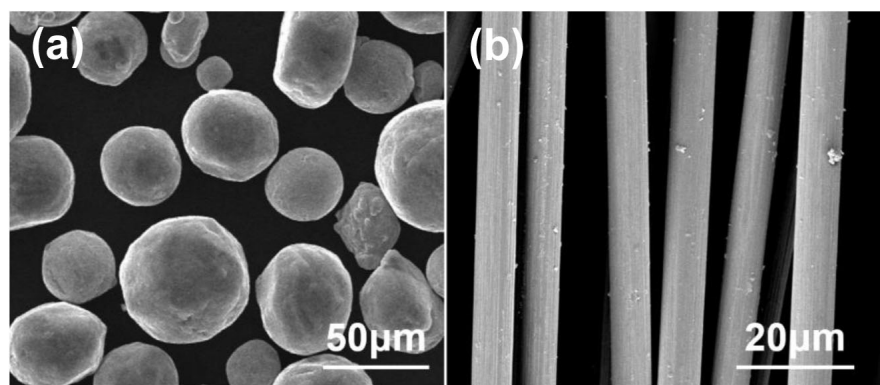


**Figure 1.** SEM images of Mg (a) and CF (b).

## 2.2. Evaluation of Microstructure and Properties

Computer tomography (CT) was performed on GE Vtomexs (240 Kv 320 W), and the microstructure of the composites was characterized by Tecnai transmission electron microscope under bright field. After grinding and polishing with sandpaper, the samples were etched with Keller reagent (HF 1 mL, HCl 1.5 mL, H<sub>2</sub>O 95 mL) for 13 s. Then the microstructure and fracture morphology were observed by optical microscope (OM) and scanning electron microscope (SEM) FEI Verios 460. The tensile test was carried out on a universal testing machine (J216) with a tensile speed of 0.5 mm/min. The tensile properties of each group of materials are based on the test results of the three samples, and the average value is taken as the final mechanical properties of the material. The tensile strength test specimens with rectangular cross-sectional area were cut by wire electrical discharge machining, and the obtained samples were named as 1.2 wt.% CF/Mg. The CT test sample was prepared by wire cutting method, and the cylindrical sample was processed into a cylinder with a size of  $\varphi 2$  mm  $\times$  8 mm. The TEM sample was prepared by slicing the wire-cut cylindrical section to a thickness of 0.3 mm, grinding to 100  $\mu$ m, and then ion thinning to 50 - 100 nm, and finally placed on a copper mesh for observation.

## 3. Results and Discussion

### 3.1. Microstructure and Composition

From **Figure 2(a)**, it can be seen that the grain of the composite material is significantly refined after the introduction of CF. This is attributed to the heterogeneous nucleation sites provided by CF increase the nucleation rate, which in turn inhibits grain growth. The samples were scanned by industrial CT to study the internal structure of the layered structure of 1.2 wt.% CF/Mg. **Figure 2(b)** shows the scanned image of the composite material. The scanning position is in the lower right corner of the image. From the color card in the picture, green and blue correspond to the distribution of carbon (C) and magnesium (Mg) elements, respectively. It can be seen that CF is layered in the Mg matrix, and the composition difference between the composite layer and the alloy layer is large.

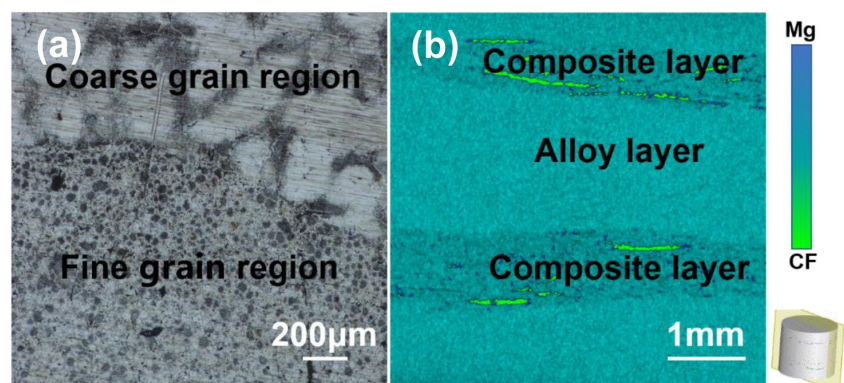


**Figure 2.** OM (a) and CT (b) image of 1.2 wt.% CF/Mg.

In the study of Ti-Al layered configuration design, Wang *et al.* pointed out that by adjusting the thickness ratio of the two layers with different mechanical properties, different mechanical properties and functional properties can be provided for the whole material, so that the properties of the material can be customized according to different application scenarios [10]. The distribution of carbon fibers in 1.2 wt.% CF/Mg samples is relatively uniform, which indicates that the synergistic effect of ball milling and sintering process effectively improves the dispersion of carbon fibers in magnesium matrix. The ball milling process can destroy the initial agglomeration structure of carbon fiber through mechanical collision and grinding. At the same time, during the sintering process, the combined effect of temperature and pressure promotes the softening and flow of the magnesium matrix, which further drives the redistribution and dispersion of carbon fibers. Provide further support for the subsequent scanned images.

**Figure 3** is the microstructure and element scanning diagram of 1.2 wt.% CF/Mg laminated composites after cooling to 530°C after the end of heat preservation and applying 12 MPa force. It can be seen that when the pressure is applied at 530°C, the higher degree of softening and more unsolidified liquid phase in the matrix make the material more prone to deformation. At this time, the thickness of the composite layer shrinks slightly, the content of CF becomes more uniform, and the interface area becomes flat. At the same time, the distribution of Mg and C elements is observed, which is further confirmed by CT results. This is because pressurization at higher cooling temperatures can increase the radius of grain boundary curvature by promoting plastic deformation, making grain boundary migration difficult and inhibiting grain growth [11].

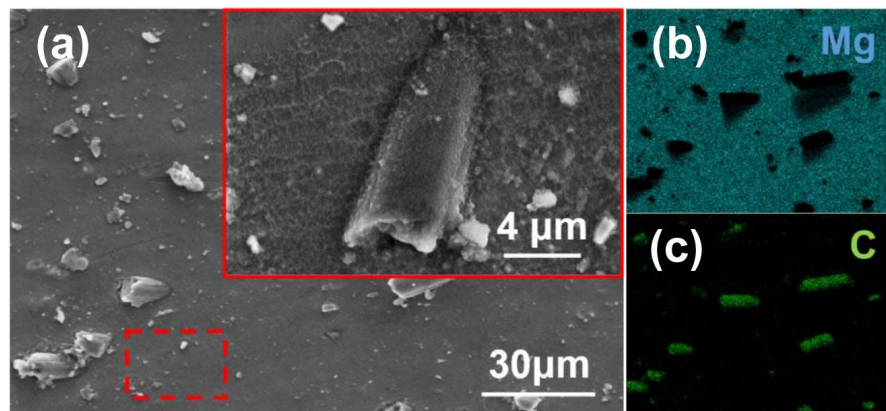


**Figure 3.** Morphology and surface scan images of 1.2 wt.% CF/Mg: (a) SEM images, (b) C element, (c) Mg element.

**Figure 4** is the X-ray diffraction pattern (XRD) of 1.2 wt.% CF/Mg laminated composites and alloys. It is worth noting that the sample of 1.2 wt.% CF/Mg exhibits a unique diffraction peak at  $2\theta = 26^\circ$ , which is a characteristic carbon peak related to the diffraction of (002) plane. In addition, no impurity phase was detected, indicating that no new phase was formed during ball milling and sintering.

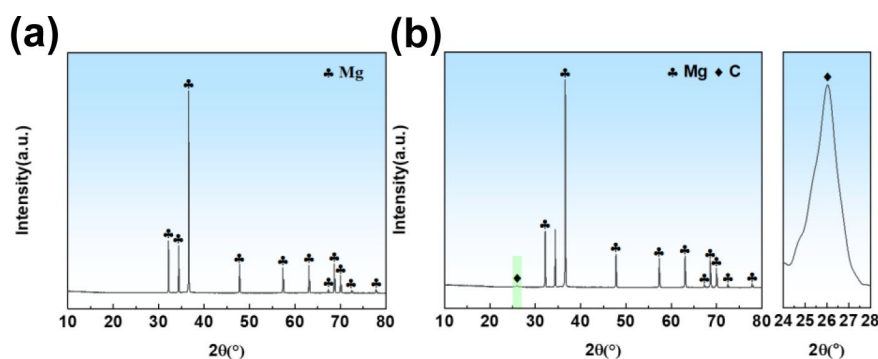


**Figure 4.** XRD patterns of different samples: (a) Mg, (b) 1.2 wt.% CF/Mg.

## 3.2. structure and Function

### 3.2.1. Structure

The composition heterogeneity of 1.2 wt.% CF/Mg was characterized by transmission electron microscopy (**Figure 5(a)**). **Figure 5(b)** is the high magnification view of 1.2 wt.% CF/Mg. From this point of view, it can be observed that some separately dispersed CFs are embedded in the matrix. It can be seen that the upper right corner of the figure is the lattice fringe obtained by the inverse Fourier transform of the marked area. The lattice spacing is ((002): 0.36 nm), and the phase can be determined to be CF. The lower right corner of the diagram is the lattice fringe obtained by the inverse Fourier transform of the marked area. The lattice spacing is ((111): 0.23 nm), which is determined to be Mg. No lattice spacing of other sizes was found near the interface, which is consistent with the conclusion obtained by XRD.

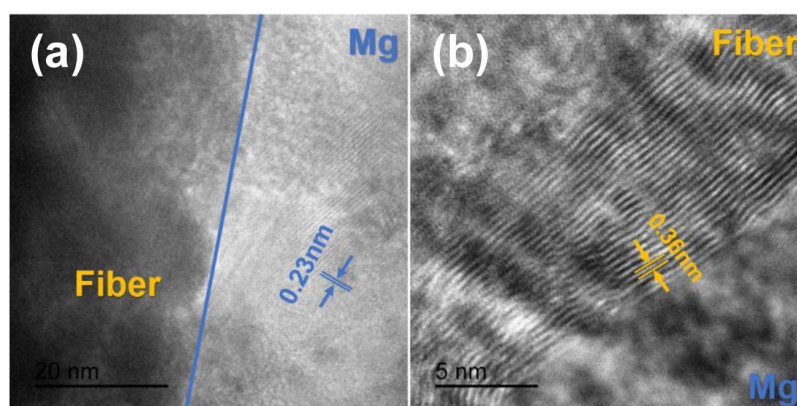


**Figure 5.** TEM images of 1.2 wt.% CF/Mg: (a) TEM morphology diagram, (b) high magnification view.

### 3.2.2. Mechanical Property

**Figure 6(a)** is the tensile stress-strain curve of magnesium alloy and 1.2 wt.% CF/Mg laminated composites sintered at 530°C. The elongation of 1.2 wt.% CF/Mg (14.7%) under this sintering process is close to that of the alloy (16.0%), and the tensile strength of the layered composite reaches 269 MPa, which is 48MPa higher than that of the alloy 221 MPa. At the same time, the strength curves of carbon materials added to some other magnesium-based materials were

compared (Figure 6(b)). This shows that the introduction of layered structure can improve the overall strength of the composite material without losing the good plasticity of the magnesium alloy matrix, and effectively solve the contradiction between strength and plasticity.

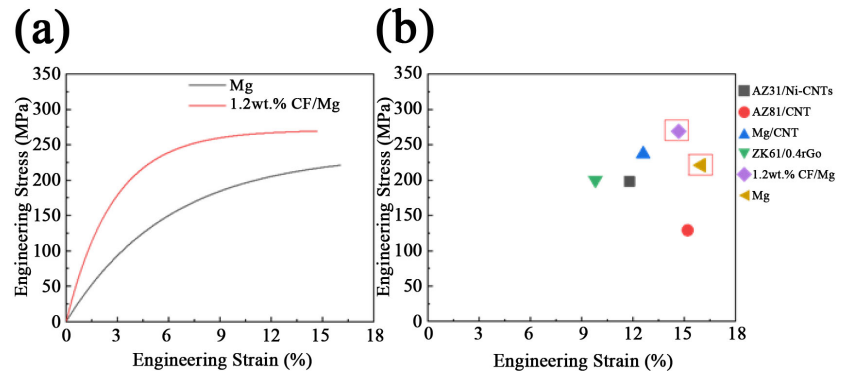


**Figure 6.** (a) The tensile stress-strain curve of Mg alloy and 1.2 wt.% CF/Mg, (b) comparison between fabricated hierarchical composite and other uniform composite [12]-[15].

### 3.3. Enhancement Mechanism of Mechanical Properties

#### 3.3.1. Strengthening Mechanism

The mechanical incompatibility between the alloy layer and the composite layer during axial tension will cause additional back stress strengthening [16]. Therefore, the strength contribution of back stress strengthening is calculated by loading-unloading-reloading tensile test [17]. The calculation formula is:

$$\sigma_b = \frac{\sigma_r + \sigma_u}{2} \quad (1)$$

where  $\sigma_b$ —back stress (MPa);

$\sigma_r$ —reloading yield stress (MPa);

$\sigma_u$ —Unloading yield stress (MPa).

This experiment is based on two key assumptions to derive the relationship between back stress, unloading yield stress and reloading yield stress [18]: First, the friction stress remains constant during unloading and reloading; second, the back stress remains unchanged before reaching the unloading yield point during unloading. Based on this, the back stress equation is established by the stress relationship at the yield point of unloading and reloading. When the stress reaches the unloading yield point, the back stress overcomes the friction stress and the applied load, which promotes the stacking dislocation to slide in the opposite direction of the stress. This will lead to:

$$\sigma_b = \sigma_u + \sigma_f \quad (2)$$

where  $\sigma_f$ —friction back stress (MPa).

Similarly, at the reloading yield point, dislocations begin to accumulate here, because the applied stress begins to overcome the back stress and friction.

$$\sigma_r = \sigma_b + \sigma_f \quad (3)$$

The back stress can be calculated by the difference between unloading and re-loading yield stress. During deformation, the alloy layer preferentially undergoes plastic deformation, and its strain is significantly higher than that of the composite layer. The strain distribution promotes the accumulation of geometrically necessary dislocations (GNDs) at the interface, resulting in a back stress opposite to the applied stress. The effective stress is the difference between the applied stress and the back stress, which needs to exceed the critical value to drive the continuous movement and accumulation of dislocations, so as to realize the strengthening of layered composites. **Figure 7** shows the unloading-reloading curve of 1.2 wt.% CF/Mg sample, and the contribution of back stress to yield strength is calculated to be 20.1 MPa. In addition, the composite also has the traditional strengthening mechanism of load transfer and grain refinement. On the one hand, CF directly bears and transmits external loads with its excellent mechanical properties, which significantly improves the strength and stiffness of composite materials. On the other hand, CF forms a stress field near the grain boundary during grain growth, which inhibits grain boundary migration and grain growth. The refined grain structure increasing the accumulation of dislocations at the grain boundaries and increases the stress required for dislocations to cross the grain boundaries, thereby further improving the yield strength of the material.

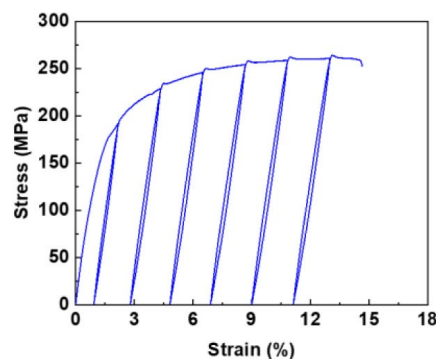


**Figure 7.** Unloading-reloading stress-strain curve of 1.2 wt.% CF/Mg.

### 3.3.2. Fracture Mechanism

**Figure 8** is the fracture SEM image of 1.2 wt.% CF/Mg laminated composite, and the “mosaic” phenomenon of CF is observed. At the initial stage of tension, the relatively uniform distribution of dimple morphology can be observed on the fracture. The heterogeneous structure inhibits strain localization through stress redistribution, and delays the premature formation of microcracks and microvoids caused by stress concentration around CF. In the second stage, micro-cracks appeared in some composite layers. The dimples and bare fibers of the alloy layer can be observed on the fracture surface. This is because when the crack propagates to the interface with the alloy layer, the alloy layer undergoes large plastic deformation, which reduces the crack growth rate and deflects the path. As the strain further increases, when the crack propagates around the CF, the CF bears the load and is gradually pulled out from the matrix. The research of David *et al.* [19]

shows that when the crack propagates around the CF, the CF can withstand the tensile stress and is gradually pulled out of the matrix. When the CF is debonded from the interface, it will consume a lot of energy and effectively delay the crack propagation. The final fracture occurs, the crack penetrates the whole material, and its propagation path shows significant passivation and deflection, which belongs to the external ductility mechanism and plays a key role in improving the ductility of the laminated composite.

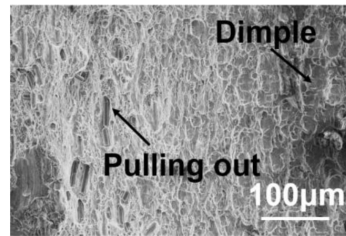


**Figure 8.** Fracture SEM of 1.2 wt.% CF/Mg.

### 3.3.3. Finite Element Simulation

In order to reduce the influence of uncertain factors on the results during the experiment, the finite element method was used to simulate the tensile behavior of the composites at room temperature. Based on the actual sample size, the corresponding tensile simulation model was established in ABAQUS software to simulate the tensile process at room temperature. The Young's modulus is 38 GPa and the Poisson's ratio is 0.3. The plastic stage is directly defined by the experimental stress-strain curve. The boundary condition is that one end is fully constrained to simulate clamping, and the other end is subjected to axial displacement load.

**Figure 9** shows the stress cloud distribution of macroscopic tensile simulation. The simulation results show that the stress is evenly distributed along the specimen at the initial stage of loading. With the increase of deformation, the stress gradually concentrates, and the specimen finally breaks at the maximum stress concentration (270.9 MPa), corresponding to the maximum strain of 15.0%. The simulation results are in good agreement with the experimental data, and the error of tensile strength simulation and elongation is within 1%. The model can better reproduce the macroscopic mechanical behavior and can be used for subsequent microscopic mechanism analysis.

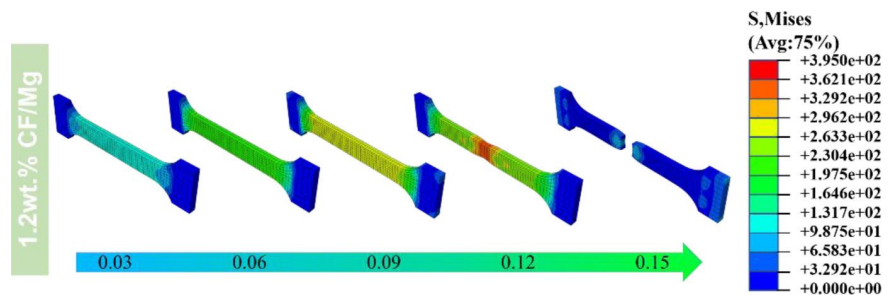


**Figure 9.** The simulation results of the mechanical properties of 1.2 wt. % CF/Mg were obtained.

## 4. Conclusions

In this paper, 1.2 wt.% CF/Mg were prepared by ball milling combined with hot pressing sintering process. The main conclusions are as follows:

1) A layered composite material with a carbon fiber-rich brittle layer as a unit was successfully prepared by ball milling and hot sintering. The interface of the obtained material is closely combined, the interlayer is smooth, and there is no obvious impurity, which provides a structural basis for giving full play to the performance of each layer.

2) Compared with the traditional magnesium matrix composites without heat treatment, the laminated composites show a significant improvement in strength and plasticity, and the strengthening and ductility mechanism is systematically explained.

3) The tensile properties of the laminated composites at room temperature were simulated. The simulation results are in good agreement with the experimental data, which verifies the reliability of the experiment.

## Acknowledgements

This work was supported by the Youth Innovation Team of Shaanxi Universities (25JP016), Shaanxi Province Qin Chuangyuan “Scientist + Engineer” Team construction (2024QCY-KXJ-112), Xianyang City Key Research and Development Program (L2025-ZDYF-KTH-004).

## Conflicts of Interest

The authors declare no conflicts of interest regarding the publication of this paper.

## References

- [1] Ouyang, M. and Li, Y. (2025) Perspectives on New Energy Revolution in China. *CSEE Journal of Power and Energy Systems*, **11**, 2623-2638. <https://doi.org/10.17775/cseejpes.2025.06840>
- [2] Yan, L. and Xu, H. (2025) Lightweight Composite Materials in Automotive Engineering: State-of-the-Art and Future Trends. *Alexandria Engineering Journal*, **118**, 1-10. <https://doi.org/10.1016/j.aej.2024.12.002>
- [3] Xu, M., Qu, J. and Li, M. (2022) National Policies, Recent Research Hotspots, and Application of Sustainable Energy: Case of China, USA, and European Countries. *Sustainability*, **14**, Article 10014. <https://doi.org/10.3390/su141610014>
- [4] Najar, F.A., Rathee, S. and Srivastava, M. (2025) Recent Advances in Friction Stir Processing of Magnesium Alloys: Microstructure, Properties, and Applications. *Metals and Materials International*. <https://doi.org/10.1007/s12540-025-02092-6>
- [5] Calado, L.M., Carmezim, M.J. and Montemor, M.F. (2022) Rare Earth Based Magnesium Alloys—A Review on WE Series. *Frontiers in Materials*, **8**, Article 804906. <https://doi.org/10.3389/fmats.2021.804906>
- [6] Qi, L., Li, S., Zhang, T., Zhou, J. and Li, H. (2019) An Analysis of the Factors Affecting Strengthening in Carbon Fiber Reinforced Magnesium Composites. *Composite Structures*, **209**, 328-336. <https://doi.org/10.1016/j.compstruct.2018.10.109>
- [7] Tuli, N.T., Khatun, S. and Rashid, A.B. (2024) Unlocking the Future of Precision

- Manufacturing: A Comprehensive Exploration of 3D Printing with Fiber-Reinforced Composites in Aerospace, Automotive, Medical, and Consumer Industries. *Heliyon*, **10**, e27328. <https://doi.org/10.1016/j.heliyon.2024.e27328>
- [8] Breish, F., Hamm, C. and Andresen, S. (2024) Nature's Load-Bearing Design Principles and Their Application in Engineering: A Review. *Biomimetics*, **9**, Article 545. <https://doi.org/10.3390/biomimetics9090545>
- [9] Wang, Y., Zhu, Y., Yu, Z., Zhao, J. and Wei, Y. (2022) Hetero-Zone Boundary Affected Region: A Primary Microstructural Factor Controlling Extra Work Hardening in Heterostructure. *Acta Materialia*, **241**, Article ID: 118395. <https://doi.org/10.1016/j.actamat.2022.118395>
- [10] Wang, Y., Du, J. and Xiao, H. (2023) Interfacial Evolution and Coordinated Deformation Mechanism of Ti/Al Laminated Metal Composites Prepared by Diffusion Bonding. *Journal of Materials Research and Technology*, **27**, 4541-4551. <https://doi.org/10.1016/j.jmrt.2023.10.264>
- [11] Rawat, N.K., Jain, N., Mishra, A.K. and Verma, A. (2024) Atomistic-Scale Simulations on Grain Boundary Migration Mechanisms Involved in Metals and Alloys: A Critical Review. *Archives of Computational Methods in Engineering*, **32**, 1931-1968. <https://doi.org/10.1007/s11831-024-10201-8>
- [12] Ding, Y., Xu, J., Hu, J., Gao, Q., Guo, X., Zhang, R., et al. (2020) High Performance Carbon Nanotube-Reinforced Magnesium Nanocomposite. *Materials Science and Engineering: A*, **771**, Article ID: 138575. <https://doi.org/10.1016/j.msea.2019.138575>
- [13] Huang, Y., Li, J., Wan, L., Meng, X. and Xie, Y. (2018) Strengthening and Toughening Mechanisms of CNTs/Mg-6Zn Composites via Friction Stir Processing. *Materials Science and Engineering: A*, **732**, 205-211. <https://doi.org/10.1016/j.msea.2018.07.011>
- [14] Wu, L., Wu, R., Zhang, J., Hou, L. and Zhang, M. (2018) Synergistic Effect of Carbon Nanotube and Graphene Nanoplatelet Addition on Microstructure and Mechanical Properties of AZ31 Prepared Using Hot-Pressing Sintering. *Journal of Materials Research*, **33**, 4261-4269. <https://doi.org/10.1557/jmr.2018.421>
- [15] Liu, F., Wang, Z., Du, X., Li, S. and Du, W. (2023) Microstructure and Mechanical Properties of Magnesium Matrix Composites Reinforced by *in Situ* Reduced Graphene Oxide. *Materials*, **16**, Article 2303. <https://doi.org/10.3390/ma16062303>
- [16] Li, X., Li, Q., Nie, M., Kong, D., Liu, Z. and Zhang, Z. (2023) Evading the Strength-Ductility Trade-Off Dilemma in Steel-Nickel Heterostructured Material by Bionic Crossed-Lamellar Structures. *Virtual and Physical Prototyping*, **18**, e2266640. <https://doi.org/10.1080/17452759.2023.2266640>
- [17] Gu, G.H., Kim, Y. and Kim, H.S. (2025) Back Stress Quantification in Heterostructured Metals: A Comparative Study of Tension-Compression and Loading-Unloading-Reloading Tests. *Materials Research Letters*, **13**, 1189-1198. <https://doi.org/10.1080/21663831.2025.2568689>
- [18] Yang, M., Pan, Y., Yuan, F., Zhu, Y. and Wu, X. (2016) Back Stress Strengthening and Strain Hardening in Gradient Structure. *Materials Research Letters*, **4**, 145-151. <https://doi.org/10.1080/21663831.2016.1153004>
- [19] David, A., Gopal, S.K., Lakshmanan, P. and Chenbagam, A.S. (2023) Corrosion, Mechanical and Microstructural Properties of Aluminum 7075—Carbon Nanotube Nanocomposites for Robots in Corrosive Environments. *International Journal of Minerals, Metallurgy and Materials*, **30**, 1140-1151. <https://doi.org/10.1007/s12613-022-2592-3>